

First Order Phase Transition of a Long Polymer Chain

by

David Aristoff and Charles Radin *

Mathematics Department, University of Texas, Austin, TX 78712

Abstract

We consider a model consisting of a self-avoiding polygon occupying a variable density of the sites of a square lattice. A fixed energy is associated with each 90° -bend of the polygon. We use a grand canonical ensemble, introducing parameters μ and β to control average density and average (total) energy of the polygon, and show by Monte Carlo simulation that the model has a first order, nematic phase transition across a curve in the β - μ plane.

November, 2010

PACS Classification: 82.35.Lr, 64.70.M-, 64.60.De, 36.20.Fz

* Research supported in part by NSF Grant DMS-0700120

1. Introduction

In polymer physics self-avoiding walks have been used for many years to model long chain molecules [1,2]. One of the oldest such models, due to Flory [3], consists of a single self-avoiding random polygon occupying *all* the sites of a square lattice, with the randomness controlled by the total energy associated with 90° -bends in the polygon. Thinking of the polygon as made of many flexibly connected monomers, the model is a canonical ensemble with the temperature behavior analyzed only at the optimally high particle density of 1. At high temperature the Flory model behaves like a disordered fluid, while at low temperature the model displays long-range nematic order. (Flory was modeling the “melting” of a nematically ordered polymer [3].) Although it is generally accepted that there is a true phase transition between these regimes in the model, there has been a dispute over the character of the transition [4], which Flory had originally predicted to be first order. For the Flory model the controversy seems to have been settled by a recent paper [5] of Jacobsen and Kondev which shows that the transition is second order. (There is a useful summary of the history of the controversy in [5].) They also suggest, however, that the transition may become first order at lower density if vacancies are permitted (see Section VII C in [5]). In our paper we concentrate on this generalization of the Flory model which allows for vacant lattice sites, so that our random polygon is now controlled by two parameters, temperature and chemical potential. We show by Monte Carlo simulation that the model has a first order phase transition. We also use order parameters to illustrate the nematic nature of the transition.

We note some other variations and applications of the Flory model. One variation uses an ensemble of polygons rather than one long polygon. Although the connection between the two models is unclear, it is of interest that there have been conflicting results on the character of the transition in this case also [6,7]. In a different direction we note that variants of the Flory model have been applied to nonequilibrium materials, specifically to crumpled or confined sheets (in 3 dimensions) and wires (in 2 or 3 dimensions). For instance in [8] we modeled a progressively confined wire in 2 dimensions by a version of the model used here, but on a triangular lattice, showing a similar transition. A field theoretic (continuum) model of a variably confined wire by Boué and Katsev [9], however, found a second order transition, and it remains to understand the origins of this difference between their continuum model and our lattice models.

2. The Model, and Results

Consider the set \mathcal{W} of all self-avoiding polygons (i.e., closed self-avoiding loops) on the square lattice with periodic boundary conditions, $L = (\mathbb{Z}/v\mathbb{Z})^2$, with v a fixed positive integer. The energy $E(w)$ of polygon w in \mathcal{W} is defined as the number of right angles in w , and the length $N(w)$ of w is the number of unit line segments in w . Given an inverse temperature $\beta = 1/T$ and a chemical potential μ , the free energy of the model is $\beta E - \beta \mu N - S(E, N)$ where $S(E, N)$ is the entropy, that is, the natural logarithm of the volume in phase space of self-avoiding polygons at fixed E and N .

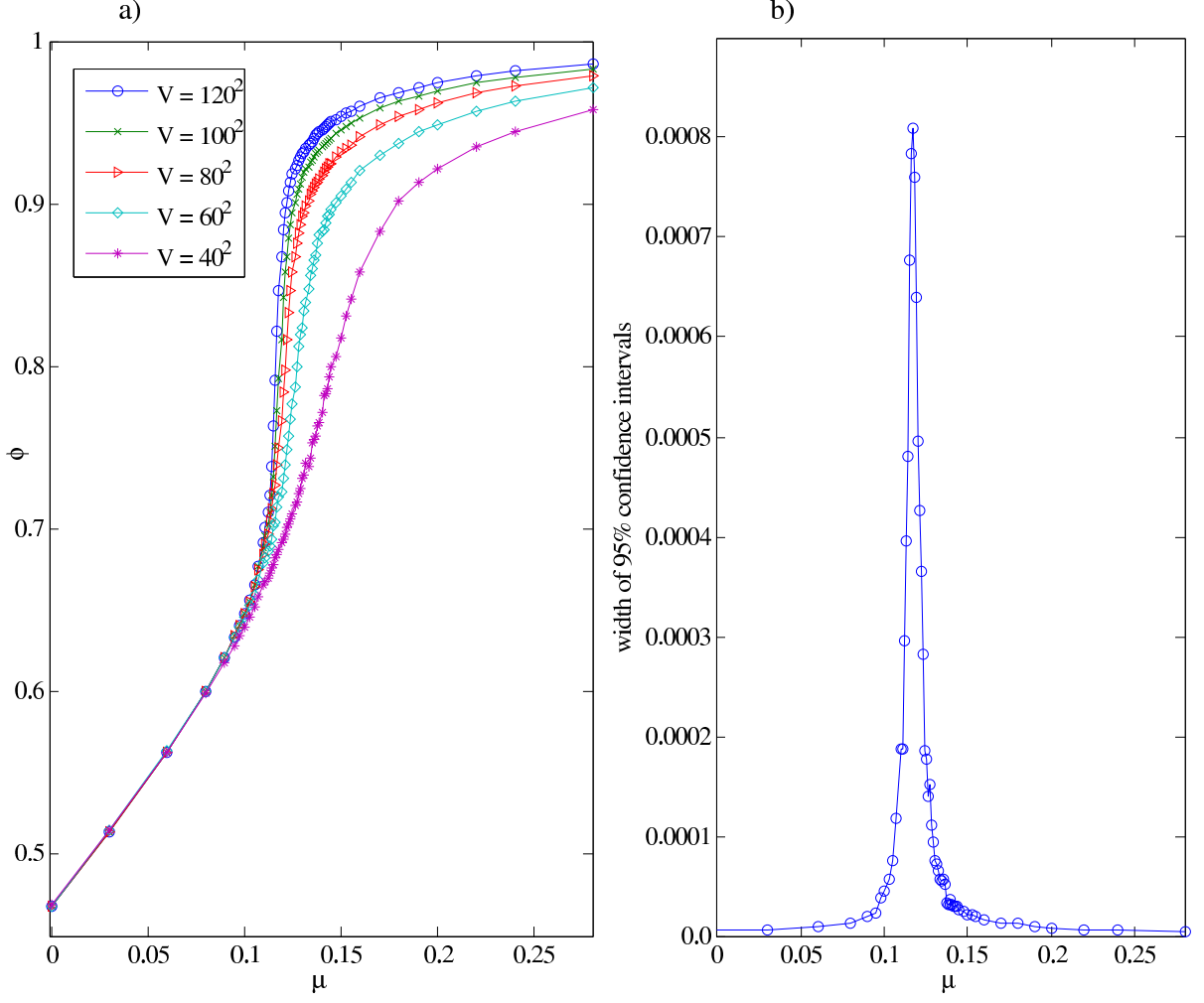


Figure 1. a) The graph of average density vs. μ at $\beta = 1.5$, for system volumes $V = 40^2$ through $V = 120^2$. b) Width of 95% confidence intervals for average density, for $V = 120^2$.

As usual in a grand canonical ensemble this is optimized by the probability measure $m_{\beta,\mu}$ defined on the subsets of \mathcal{W} by

$$m_{\beta,\mu}(w) = \frac{1}{Z_{\beta,\mu}} e^{-\beta(E(w) - \mu N(w))}, \quad 1)$$

for $w \in \mathcal{W}$, where $Z_{\beta,\mu}$ is the appropriate normalization. In this notation we have suppressed the dependence of $m_{\beta,\mu}$ and $Z_{\beta,\mu}$ on the system volume $V = v^2$.

To simulate the model we fix either β or μ , and then slowly increase the other parameter, starting from well into the disordered regime. The basic Monte Carlo step is as follows (see pgs. 41-44 in [10]). Given a polygon $w(t)$ at step t in the simulation, we introduce, with probability p_i , a trial configuration $w(t)'$ which changes the length of $w(t)$ by ℓ_i . If $w(t)'$ is not self-avoiding then we take $w(t+1) = w(t)$; otherwise

we set $w(t+1) = w(t)'$ with probability $q = \min(Q, 1)$, and $w(t+1) = w(t)$ with probability $1 - q$, where

$$Q = e^{\beta[\mu\ell_i + E(w(t)) - E(w(t)')]} \quad (2)$$

Here $p_1 = p_2 = 2/5$, $p_3 = 1/5$, $\ell_1 = -2$, $\ell_2 = 2$ and $\ell_3 = 0$.

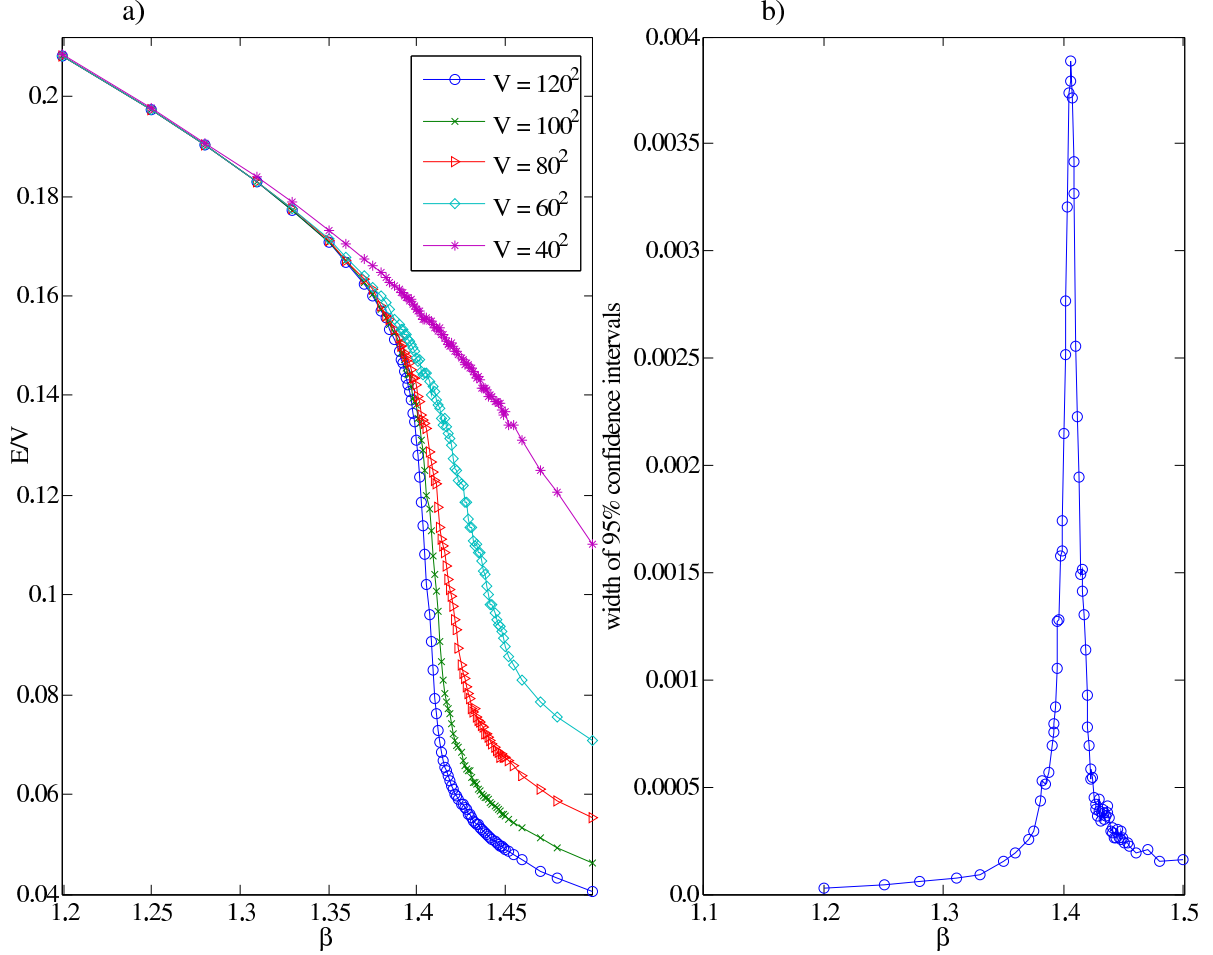


Figure 2. a) The graph of average energy per volume vs. β at $\mu = 0.15$, for system volumes $V = 40^2$ through $V = 120^2$. b) Width of 95% confidence intervals for average energy per volume, for $V = 120^2$.

To determine whether the simulation for each pair (β, μ) has sufficiently many Monte Carlo steps, we compute a “mixing time” as the smallest t such that the standard autocorrelation function

$$\frac{1}{(n-t)\sigma^2} \sum_{i=1}^{n-t} (meas(w_i) - \lambda) \cdot (meas(w_{i+t}) - \lambda) \quad (3)$$

falls below zero. Here $meas$ represents any of our various measurements, described below, λ and σ^2 are the sample average and variance (respectively) of $meas$ over the

simulation of (β, μ) , and w_i is the i th configuration in the simulation of (β, μ) , with n total steps. We found that our simulations of each (β, μ) were, in the worst cases, at least 5 mixing times long (on average), and we therefore believe our Monte Carlo runs are reasonably close to sampling the distributions $m_{\beta, \mu}$. We repeated each of our simulations 100 times, and obtained 95%-confidence intervals for $meas$ from Student's t -distribution with 99 degrees of freedom on the average values of $meas$ over each simulation. (Measurements related to specific heat were calculated differently, and are discussed below.) A single simulation of the largest system ($V = 120^2$) contains 8×10^{11} basic Monte Carlo steps.

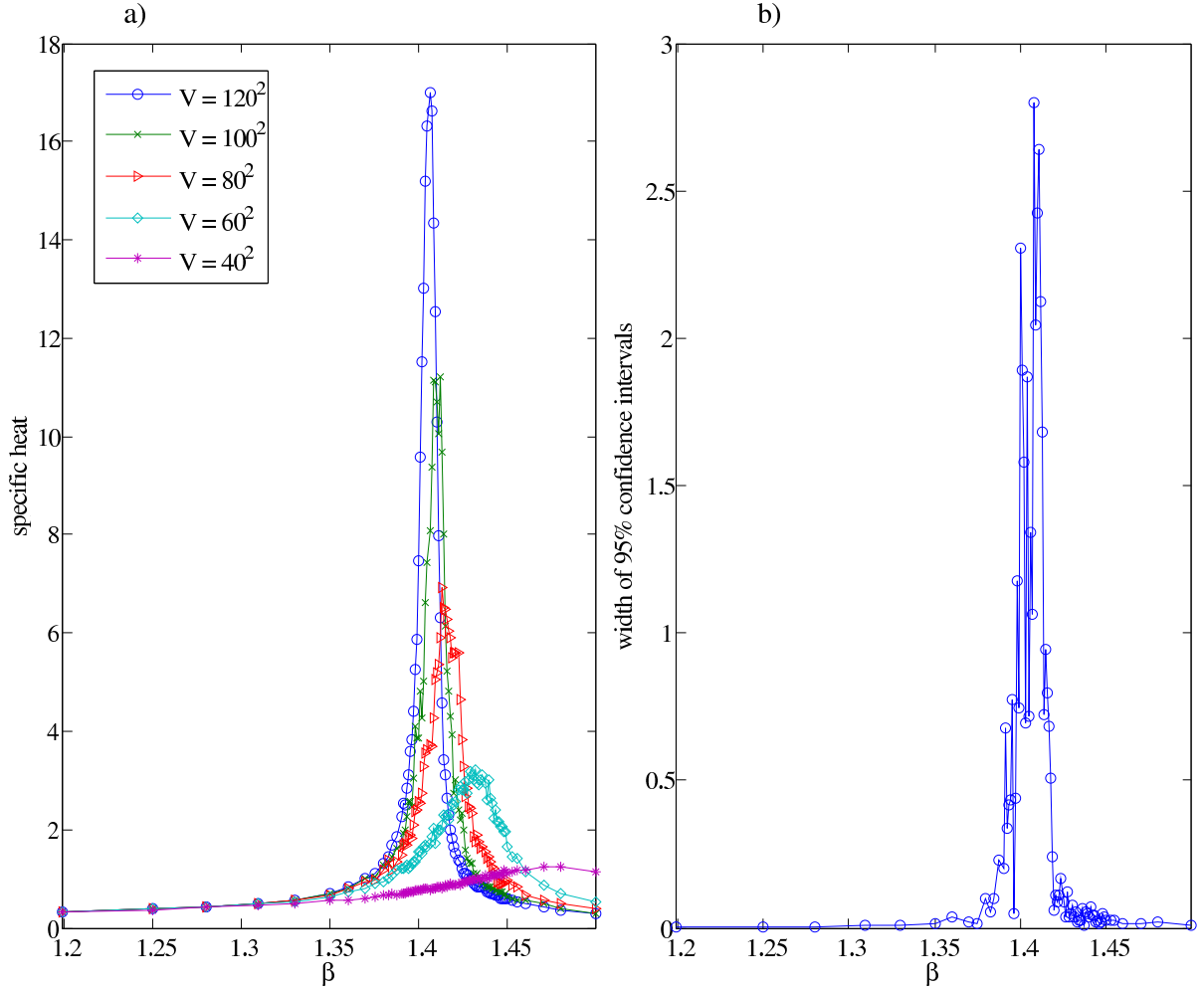


Figure 3. a) The graph of specific heat vs. β at $\mu = 0.15$, for system volumes $V = 40^2$ through $V = 120^2$. b) Width of 95% confidence intervals for specific heat, for $V = 120^2$.

We measure average energy per volume $\langle E \rangle_{\beta, \mu} / V$, average density $\langle \phi \rangle_{\beta, \mu}$, as well as order parameters $corr$ and lay , which were introduced in [8] and are defined as follows. Given a polygon w , $corr(w)$ is the proportion of edges in w which have the

same orientation (horizontal or vertical) as a randomly chosen edge in w . Given w , $lay(w)$ is the normalized volume u^2/V of the largest square sublattice $L' = (\mathbb{Z}/u\mathbb{Z})^2 \subset L$ such that the orientation of w (horizontal or vertical) at the origin agrees with the orientation of w at 80% or more of the sites in L' . (We choose an orientation for the polygon w so that each lattice site has a unique horizontal or vertical orientation.)

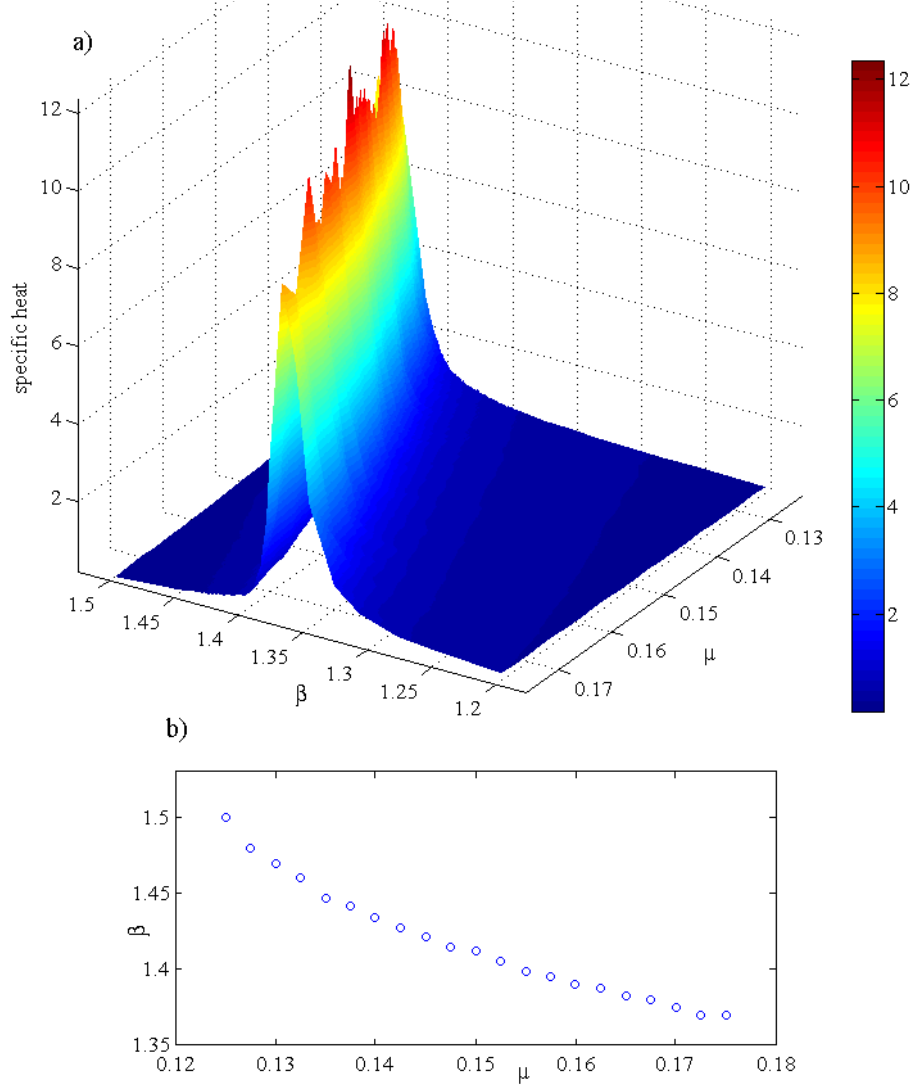


Figure 4. a) The graph of specific heat vs. β and μ , for $V = 100^2$. b) Estimation of β values which maximize specific heat at fixed μ .

We compute specific heat $(1/V)\partial\langle E\rangle_{\beta,\mu}/\partial T$ from fluctuations, that is,

$$T^2 \frac{\partial\langle E\rangle_{\beta,\mu}}{\partial T} = \langle E\rangle_{\beta,\mu} \langle \mu N - E\rangle_{\beta,\mu} - \langle E\mu N - E^2\rangle_{\beta,\mu}. \quad (4)$$

To compute the values of $\langle \cdot \rangle_{\beta,\mu}$ from equation (4), we took averages of the relevant

measurements *meas* over 100 independent simulations. Then for 95%-confidence intervals we repeated this process 4 times, and used the Student's *t*-distribution with 3 degrees of freedom. We checked that the resulting curve agreed with the numerical derivative of energy.

In contrast with [8] we simulate well into the ordered regime and find direct evidence of a first order phase transition. In particular the trends with increasing system size in the curves of Figs. 1 and 2 strongly suggest that the average density and average energy per volume both develop jump discontinuities at the transition, in the infinite volume limit. In confirmation, Fig. 3 shows the specific heat developing a delta function singularity at the transition.

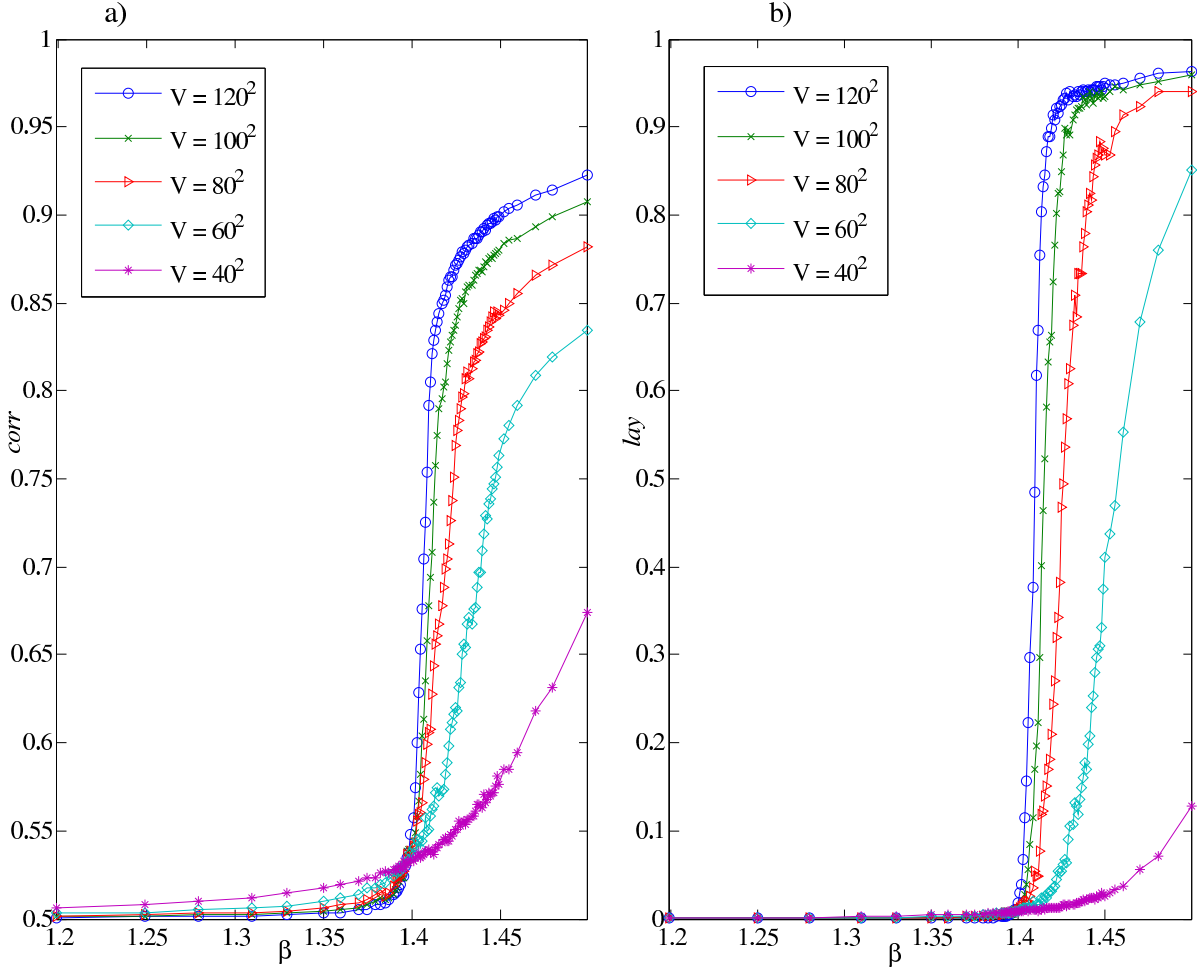


Figure 5. a) The graph of $corr$ vs. β at $\mu = 0.15$, for volumes $V = 40^2$ to $V = 120^2$. b) The graph of lay vs. β at $\mu = 0.15$, for volumes $V = 40^2$ to $V = 120^2$.

We plot the specific heat surface as a function of β and μ , as well as the (β, μ) -coordinates of the maximum of specific heat, at various $0.125 \leq \mu \leq 0.175$, $1.2 \leq \beta \leq 1.5$ in Fig. 4. The latter gives an indication of the transition curve; note that as μ

increases, the temperature at which the transition occurs increases.

As evidence of an nematic transition, the measurements *corr* and *lay* (see Figs. 5 and 6) exhibit a jump discontinuity at the transition from their disorder values of 1/2 and zero, respectively.

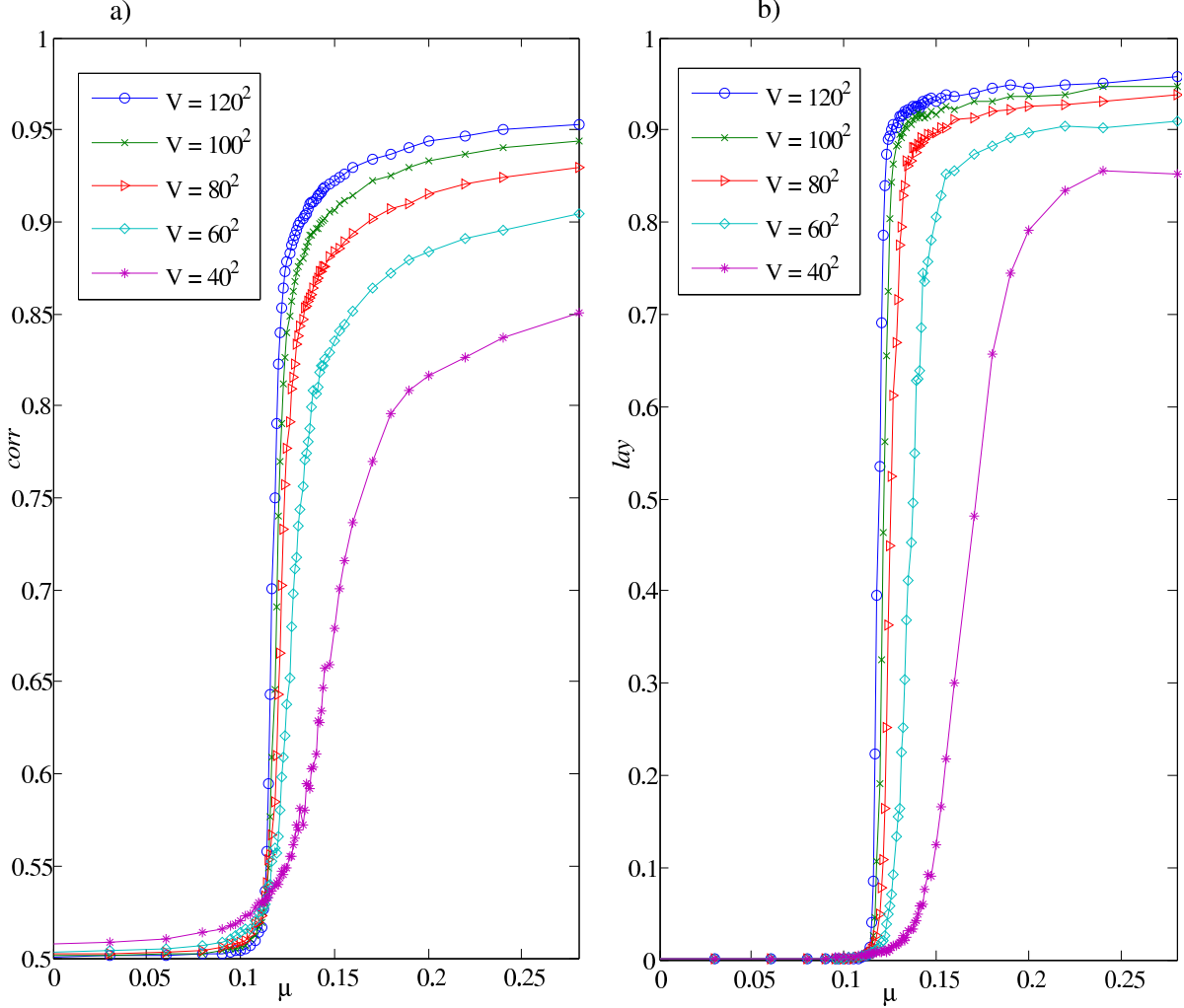


Figure 6. a) The graph of *corr* vs. μ at $\beta = 1.5$, for volumes $V = 40^2$ to $V = 120^2$. b) The graph of *lay* vs. μ at $\beta = 1.5$, for volumes $V = 40^2$ to $V = 120^2$.

3. Nonequilibrium

We mentioned above that with variable density added, a version of the Flory model on a triangular lattice has been used [8] to model wires progressively confined in 2 dimensions. (See [11] for a related approach, and further references.) We add here a note on the modeling of such nonequilibrium materials. Since the polygons are self-avoiding, these lattice models introduce a unit length scale for the width of the wire. Now if it requires energy E to bend one wire of unit thickness to a given radius of

curvature it would require mE to bend a loose bundle of m parallel wires, but because of the interconnectedness it would require more than mE to bend a single wire of thickness m . Therefore the bending energy is highly nonlinear in the thickness of the wire, growing faster than the square of the thickness, and so energy is an independent parameter in our modeling.

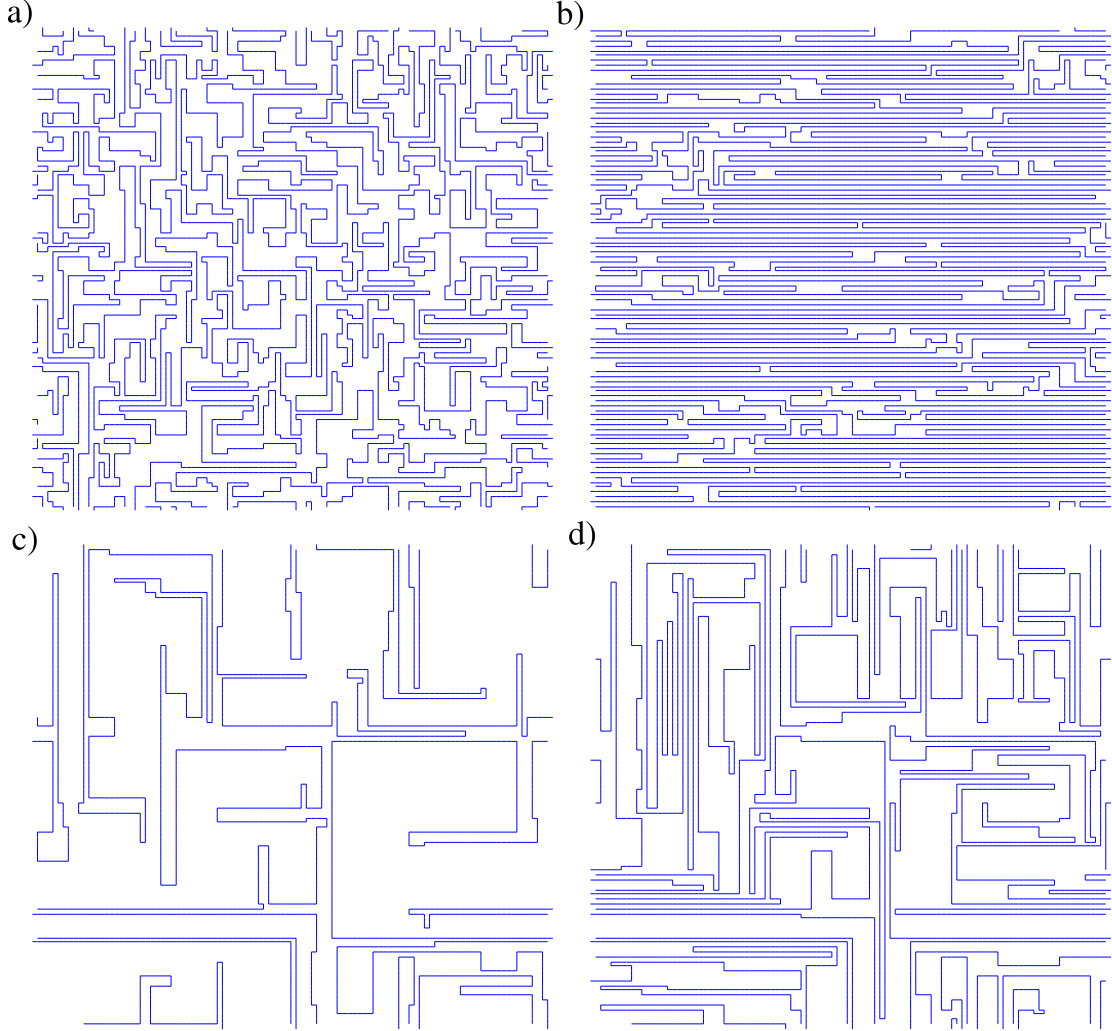


Figure 7. Configurations with $V = 100^2$ in equilibrium at:

- a) $(\beta, \mu) = (1.5, 0.03)$ and density $\phi = 0.392$
- b) $(\beta, \mu) = (1.5, 0.13)$ and density $\phi = 0.655$,
- c) $(\beta, \mu) = (2.5, 0.01)$ and density $\phi = 0.146$,
- d) $(\beta, \mu) = (2.5, 0.025)$ and density $\phi = 0.392$.

Fig. 7 shows typical polygons with low and high volume fraction, but at two very different temperatures. This could be useful in estimating whether experimentally

confined materials are in an ordered or disordered regime. An alternative method would be to compute order parameters such as *lay* or *corr*.

4. Conclusion

We have introduced a version of the Flory model that allows for a positive fraction of vacancies, and shown by Monte Carlo simulation that the model has a first order, nematic phase transition. In terms of the (inverse) temperature β and chemical potential μ of our grand canonical ensemble, we find that the transition lies approximately on the curve shown in Fig. 4 b).

We conclude by contrasting the results in this paper with those in [8], which uses a very similar model, but on a triangular lattice and therefore with greater complexity of the interaction energies. A grand canonical ensemble was also used in [8], but simulations were confined to a single isotherm.

The evidence in [8] of a nematic transition is based on two order parameters, *lay* and *corr*, used also in this paper. The arguments in [8] are based heavily on trends in these order parameters as the system size is increased, namely that at low chemical potential μ both order parameters decrease monotonically toward their disordered values, while at higher μ both order parameters increase monotonically away from their disordered values. This strongly suggests a nematic transition, which would be expected to be first order. The simulations in [8] became unreliable moving into the ordered regime, so in particular no direct evidence was given of a discontinuity of a first derivative of the free energy, namely volume fraction or energy density.

For the present paper, which also reports a nematic transition in a model similar to [8] but on a square lattice, as in the original Flory model [4,5], we were able to make reliable simulations well into the ordered regime, and simulated on a grid of values of μ and β . The main improvement over [8] is that now we are able to show discontinuities in volume fraction and energy density, the usual hallmarks of a first order transition, as well as discontinuities in *corr* and *lay*, which clarify the nematic nature of the transition. We feel this is strong, direct evidence supporting the suggestion in [5] that the second order transition which they find at density 1 in the Flory model becomes first order at lower density when vacancies are included in the model. It still remains to reconcile this behavior with that found in [9] in their continuum model of confined loops.

Acknowledgements. We are grateful to E. Katzev, S. Deboeuf, A. Boudaoud and N. Menon for useful discussions.

References

- 1 P.J. Flory, *Statistical Mechanics of Chain Molecules*, Wiley, 1969.
- 2 P.-G. de Gennes, *Scaling Concepts in Polymer Physics*, Cornell University Press, Ithaca, 1979.
- 3 P. J. Flory, Proc. R. Soc. London, Ser. A 234, 60 (1956).
- 4 G. I. Menon and R. Pandit, Phys. Rev. E 59, 787 (1999).
- 5 J. L. Jacobsen and J. Kondev, Phys. Rev. E, 69 (2004) 066108.
- 6 J. F. Nagle, Proc. R. Soc. London, Ser. A 337, 569 (1974).
- 7 A. Baumgartner and D. Yoon, J. Chem. Phys. 79, 521 (1983).
- 8 D. Aristoff and C. Radin, Europhys. Lett. 91 (2010) 56003.
- 9 L. Boué and E. Katzav, Europhys. Lett. 80 (2007) 54002.
- 10 E.J. Janse van Rensburg, J. Phys. A 42 (2009) 323001.
- 11 M. Adda-Bedia, A. Boudaoud, L. Boué and S. Deboeuf, arXiv:1009.1001v1.